Predicting the Functional Motions of p97 Using Symmetric Normal Modes

Hyuntae Na,[1] and Guang Song[1,2,3*]

[1]Department of Computer Science,

[2]Program of Bioinformatics and Computational Biology,

[3]L. H. Baker Center for Bioinformatics and Biological Statistics,

Iowa State University, Ames, IA 50011, USA

*Correspondence to: Guang Song, Tel: 515-294-1696;

Fax: 515-294-0258; E-mail: gsong@iastate.edu

September 7, 2016

Running title: Functional Motions of p97 by Symmetric Modes

Key words: symmetry; pore loop; threading; mechanism; dynamics; cooperativity

Abstract

p97 is a protein complex of the AAA+ family. Though functions of p97 are well understood, the mechanism by which p97 performs its unfolding activities remains unclear. In this work, we present a novel way of applying normal mode analysis to study this 6-fold symmetric molecular machine. By selecting normal modes that are axial symmetric and give the

largest movements at D1 or D2 pore residues, we are able to predict the functional motions of p97, which are then validated by experimentally observed conformational changes. Our results shed light and provide new understandings on several key steps of the p97 functional process that were previously unclear or controversial, and thus are able to reconcile multiple previous findings. Specifically, our results reveal that i) a venous valve-like mechanism is employed at D2 pore to ensure a one-way exit-only traffic of substrates; ii) D1 pore remains shut during the functional process; iii) the "swing-up" motion of the N domain is closely coupled with the vertical motion of the D1 pore along the pore axis; iv) because of the shut D1 pore and the one-way traffic at D2 pore, it is highly likely that substrates enter the chamber through the gaps at the D1/D2 interface. The limited chamber volume inside p97 suggests that a substrate may be pulling out from D2 while at the same time being pulling in at the interface. v) Lastly, p97 employs a series of actions that alternate between twisting and pulling to remove the substrate.

1 Introduction

Eukaryotic p97 is an important protein in the extended AAA (ATPases Associated with diverse cellular Activities) family and it plays a key role in ubiquitin-dependent cell signaling and degradation. Many studies[31,32,39] have been carried out to determine its roles in ERAD, or endoplasmic reticulum-associated degradation. It is also known as VCP, or valosin-containing protein, or Cdc48 in yeast.

P97 is a 6-fold symmetric homo-hexamer (see Figure 1). Each unit has a N domain, a D1 and a D2 domain that are ATPases, and a C-terminal strand that has a role to identify and bind with other complexes[3]. It has a central pore, which is widely believed to be critically important for substrate processing, possibly by threading.

Though the functions of p97 have been well understood, the mechanism by which it realizes its function is less clear and controversial. About a dozen of high-resolution structures of p97 have been determined in the last decade or so[2,11,18,20], see Table I. These structures provide a rich understanding of the atomic structure of p97, but the mechanism remains unclear.

Sequence wise, D2 pore loop residues are found to be mostly conserved[33]. D1 pore loop

residues, on the other hand, are not conserved (see Figure 1 of Ref. 33).

A number of models exist for p97 regarding how it functions. These models differ significantly from each other[4]. One of them is the threading model. In this model, it was thought that N domain recognizes and binds substrates and then the substrate is threaded into the chamber from D1 pore and threaded out at D2 pore. Indeed, there exist some AAA+ unfolding machines that function in this way[17], such as bacterial ClpA/ClpP[21], Pex1/6[10,15], etc. Later on, however, crystal structures of p97 by Brunger and co-workers showed that D1 pore is blocked by HIS 317[12,13]. Through mutation studies, Brunger and co-workers[14] showed that many residues along D2 pore are important to the degradation. In contrast, the same authors[14] found that mutations (except for H317A) at D1 pore does not alter degradation, suggesting that D1 pore was not used for translocation. As for the single mutation H317A that significantly affected degradation, the interpretation was that H317 serves to provide a strong nexus to ensure the cooperativity among the protomers and mutation H317A disrupts the needed cooperativity and consequently the proper functions of p97[14]. Their results thus provide strong evidence that D1 pore remains shut the whole time during the functional process. The author then proposed that substrates may interact or even enter the p97 chamber through D2 pore and then come out of it in the same way, though it seems unlikely since the small size of the chamber makes it unlikely for the whole substrate to turn around. The author proposed also an alternative model in which the substrate may exit through gaps at the interface between D1 and D2 domains, though there was no much evidence to support this claim.

Another evidence that D1 pore may not be active is that the D1 pore of eukaryotic p97 does not have any aromatic residues. The presence of aromatic residues in the central pore is considered to be important to the unfolding activity of AAA+ unfoldases. At least one aromatic residues were found in bacterial Alp family and archaeal VAT protein[33]. Other evidence that supports a closed D1 pore is that all 13 existing structures (see Table I) of p97 in the PDB have a closed D1 pore.

Evidence supporting the possible existence of an open D1 pore also exists. For example, Rothballer et al.[33] found that if the aliphatic residues leucine and alanine of the D1 pore are replaced with aromatic tyrosine and the N domain is also removed, the truncated and mutated p97 displays unfolding[33] and degrading capability[3]. These results suggest that the D1 domain of p97 may still

possess the translocation-based unfolding capability. Furthermore, recent cryo-EM based studies by Yeung et al.[40] showed that p97 has an open D1 pore at the apo conformation. What is most unique about the work by Yeung et al.[40] from others is that they observed *a 3-layer architecture* of p97, which none of published structures up to that time had. However, the most recent published work by Banerjee et al.[2] confirmed the existence of such a 3-layer architecture, by reporting a similar structure at ATP bound state.

Another outstanding feature of p97 is the relative rotational twisting between D1/N domains and D2 domain, which has been observed in some other AAA+ structures as well[8]. This rotation has been clearly observed in both atomic force microscopy (AFM) based studies[30] and cryo-EM based studies[40]. The two most recent atomic structures of human p97[2,18] both found a conformation at such a rotated state. There is little doubt thus this twisting motion should be functionally important.

Yet another outstanding feature of this 6-fold symmetric molecular machine is the strong cooperativity among the functionally active D2 domains[14] of its six protomers. In the recently reported work[2], all three conformations (pdb-ids: 5FTL, 5FTM, 5FTN) are axial symmetric, which strongly indicates that ATP binding and hydrolysis at the six units may synchronize allosterically. Indeed, Banerjee et al.[2] observed from analyzing cryo-EM images that "Analysis of the images without imposition of 6-fold symmetry shows that the majority of the molecules are in one of the three conformations obtained with the use of symmetry, indicating that the structural changes between conformations I, II and III are cooperative in nature"[2]. Therefore, it is reasonable to presume that p97 remains axially symmetric during the functional process. This is consistent with the aforementioned experimentally-observed inter-ring rotations, which also demonstrate axial symmetry.

Based on this presumption, in this work we present a novel way of applying normal mode analysis to study this 6-fold symmetric molecular machine. By selecting normal modes that are axial symmetric and give the largest movements at D1 or D2 pore residues whose motions are known to be critically important to substrate processing, we are able to predict the functional motions of p97, which are then validated by experimentally observed conformational changes. Our results shed light on and provide new understandings into several steps of the mechanistic process

that were unclear and controversial, and thus are able to reconcile and bring together multiple previous findings.

2 Methods

2.1 Normal Mode Analysis

Normal mode analysis, or NMA in short, was first applied to study the vibrational motions of proteins in early 80's[7,16,22,35]. The classical NMA, or CNMA, uses an all-atom force-field that may have hundreds of parameters. To run CNMA, the input structure has to be energetically minimized according the force field potential. Then the second derivatives of the potential relative to the general coordinates can be computed, from which eigenvalues and eigenvectors (modes) can be obtained.

Normal mode analysis can be carried out also using simplified potentials and/or simplified structure models. There exists a tight link between the classical NMA and simplified NMA models[23–25].

2.2 Spring-based NMA

In 2014, we realized that the Hessian matrix of the CNMA could be written a summation of spring-based terms and force-based terms and the force/torque-based terms contributed significantly less than the spring-based terms[24,25]. We thus developed a new model called spring-based NMA, or sbNMA[24], that keeps only the spring-based terms of the Hessian matrix of classical NMA. There are two significant advantages of sbNMA over CNMA. First, it does not require energy minimization and thus can be applied to experimental structures directly[24]. Second, it is superior to other simplified models such as ANM[1] in that it is highly accurate and closely resembles CNMA: sbNMA gives a high correlation with CNMA in mean square fluctuations (close to 0.9 on average, while ANM's average correlation with CNMA was 0.46 for the dataset used.[24]) and is able to reproduce vibrational spectra given by CNMA with high accuracy[29].

2.3 Structures

In this work, we use three atomic-resolution conformations that are determined simultaneously using cryo-ENM[2]. There are conformation I (ADP bound at both D1 and D2 domains, pdb-id: 5FTL), conformation II (ADP bound at D1 while ATPγP bound at D2, pdb-id: 5FTM), and conformation III (ATPγP bound at both D1 and D2 domains, pdb-id: 5FTN). See also Table I.

2.4 Symmetric Normal Modes

p97 has a 6-fold axial symmetry. We compute the symmetricity of each mode as follows. For each mode M_i,

$$M_i = \begin{bmatrix} \mathbf{u}_1 \\ \mathbf{u}_2 \\ \vdots \\ \mathbf{u}_5 \\ \mathbf{u}_6 \end{bmatrix} \tag{1}$$

where $\mathbf{u}_i$ represents the mode components of the ith subunit, we perform a rotation along the pore axis by $\frac{2\pi}{6}$. The pore axis of p97 is determined by connecting the geometric center of the C_α atoms of pore residues Leu278 (six of them, out of the six subunits) at the D1 domain and that of pore residues Trp551 at the D2 domain. Let R represent this rotation in a 3 by 3 matrix form. Let M_i' be the mode after the rotation. M_i' has the following form,

$$M_i' = \begin{bmatrix} (I_n \otimes R)\mathbf{u}_6 \\ (I_n \otimes R)\mathbf{u}_1 \\ \vdots \\ (I_n \otimes R)\mathbf{u}_4 \\ (I_n \otimes R)\mathbf{u}_5 \end{bmatrix} \tag{2}$$

where $\otimes$ represent kronecker product and I_n is an indentity matrix of size n and n is the size of each subunit. M_i' takes the above form because after the rotation the first subunit takes the spot of

the second, the second takes the spot of the third, and so on. Notice that this formulation can be straightforwardly generalized and extended to any complex with n-fold axial symmetry.

The symmetricity of mode i is defined as the overlap (or dot product) between M_i and M_i',

$$symmetricity = M_i \cdot M_i'. \tag{3}$$

If a mode is perfectly symmetric along the pore axis, the rotation has no effect and its symmetricity should be 1. That is, the mode is invariant under the rotation. The level of symmetricity reveals how similar the motions of adjacent subunits are, or the extent to which adjacent subunits move together.

3 Results

To uncover the mechanism of p97, we carry out a normal mode analysis of p97 using recently determined high-resolution cryo-EM structures[2]. We employ the sbNMA model[23,24,26,27]. The advantage of sbNMA is that it is highly accurate, closely resembling the classical all-atom NMA. Yet at the same time, it does not require energy minimization.

To apply the sbNMA, the structure is first protonized. This is done by using the psfgen program in VMD[19]. The position of the hydrogen atoms are then energetically minimized. After this, the all-atom sbNMA Hessian matrix is constructed. It is then projected to coarse-grained space while preserving the accuracy of the dynamics [23].

3.1 The Layout of p97 Pore at the Static Structures

To obtain the pore layout of p97 at different nucleotide binding states, we use the near-atomic structures recently determined by Banerjee et al.[2] Figure 2 shows a cross section view of the layout of D1 and D2 pores and the internal chamber of p97. It is seen that D1 pore is closed at all three states and that D2 pore is nearly closed when ATPs are bound at both D1 and D2 domains (conformation III of Banerjee et al., pdb-id: 5FTN). The internal volumes between the two narrow necks of the pore is about 24,000 Å^3 at ADP/ADP bound state (conformation I), 16,000 Å^3 at

ADP/ATP bound state (conformation II), and 17,000 Å^3 at ATP/ATP bound state (conformation III). Therefore, after ATP hydrolysis at the D2 domain, the internal volume increases by about 50%.

3.2 Symmetric Normal Modes

A common challenge of applying NMA to decipher the mechanism of a protein system is how to decide which modes are functionally important, as there are many of them. Visually inspecting the modes one by one is tedious and arbitrary.

Thankfully, the recently published structures determined by Banerjee provide a helpful guidance, as the authors determine the structure of p97 at different nucleotide-bound states, namely, ADP bound (conformation I), ADP and ATP bound (conformation II), and ATP bound (conformation III). The layout of the pore at conformations I, II, and III as given in Figure 2 reveals that the D1 pore is mostly closed. However it is difficult to infer mechanism from these static structures alone.

Though these conformations do not represent the full conformation space, they do represent some of the most favorable conformations. All three conformations are axial symmetric, which indicates that ATP hydrolysis may synchronize allosterically. Therefore, it is reasonable to presume that p97 remains mostly axially symmetric in its functional process. The rest of our studies are based on this presumption. we identify all the modes that are axial symmetric. We skip non-symmetric modes since it can be shown that for a perfectly symmetric ring structure with n subunits, $1/n$ of the modes are fully symmetric[34] (i.e., symmetricity=1) and these symmetric modes form a closed subspace, which represents all and only the motions that are axially symmetric. Consequently, any other non-symmetric modes cannot be combined to form symmetric modes even if they have identical or nearly identical eigenvalues. While this is no longer the case when a structure starts to deviate from the perfect symmetry, since some of the $1/n$ modes that used to be fully symmetric may become degenerate[28] and lose some of their symmetricity, symmetric modes that are functional are likely conserved. They generally are of low frequency and are robust to degeneracy, and can thus maintain their symmetricity. Therefore it is still reasonable to focus only

on symmetric modes.

Figure 3 plots the distribution of the extent of symmetry of the modes. Only a small percentage of the modes are highly symmetric according to our definition of symmetricity (which is given in the Methods section).

3.3 Identifying the Functional Modes

Studies[14] have shown that the functions of p97 are closely linked to the D2 pore residues, and to a much lesser extent, D1 pore residues. N domains are known to be very flexible and are thought to involve in the recognition of the substrates. It was thought that D2 pore residues may serve as a clamp that grabs an substrate and drags it out from the chamber, as some other proteins in the AAA+ family do. Indeed, D2 pore utilizes two conserved hydrophobic residues Trp551 and Phe552[33]. For D1 pore, early studies using crystallography showed that HIS 317 is the residue that blocks the D1 pore[12,13]. Mutation studies found that HIS 317 was essential to substrate interaction and endoplasmic reticulum-associated degradation (ERAD)[14].

For this reason, we identify *axial symmetric modes that give the largest movements at these pore residues* (TYR 551 and PHE 552 for D2 pore and HIS 317 for D1 pore). By movement we mean the squared fluctuation (SF) contributed by a given mode (say mode i), weighted by the mode's eigenvalue λ_i, i.e., $(\Delta x^2 + \Delta y^2 + \Delta z^2)/\lambda_i$. (The average of these squared fluctuations is the commonly computed mean-square fluctuations, or MSF). To find the modes that give the largest movements (or SFs) at a given residue, say TYR 551, we compute the SFs at TYR 551 by each and every mode and sort them. We then pick the top k modes that give the largest SFs at TYR 551. We hypothesize that these modes should be functional and should reveal the *key actions* of the pore residues as well as those of the rest of the protein in the functional process. The results are given in Tables II and III, which list top ten modes that have the largest movements at D1 and D2 pore residues. The squared fluctuations along the X-Y plane (transverse direction) as well as the directions of motions of the pore residues as denoted by θ and ϕ (see Figure 4 for an illustration) also are listed. The direction of motion as represented by θ and ϕ is helpful as it indicates what kind of motion a mode has: longitudinal (small θ), radial ($\theta \approx 90°$ and small ϕ), or tangential

($\theta \approx 90°$ and $\phi \approx 90°$).

A few interesting observations stand out. First, mode 13 clearly gives the largest movement at D2 pore residues W551 and F552. And the movement is mostly longitudinal along the pore (θ is close to 0°). Mode 41 on the other hand, gives the largest movement in the transverse direction and has basically no vertical movement. Therefore mode 41 represents an stretching open/close motion of the pore. However the scale of motions of mode 41 is more than 25 times smaller than mode 13. Mode 7 is a transverse motion (its θ value is about 90°) and more precisely, it is mostly a rotational motion (its ϕ value is about -80 °). For the same mode 7, the pore residue H317 at D1 pore is rotating in the opposite direction ($\phi = 72°$). Thus mode 7 may represent a twisting motion.

For D1 pore, mode 4 gives the largest movement at D1 pore residue HIS 317. Compared with the modes identified for D2 pores, a striking phenomenon is that none of the modes identified for D1 pore has a significant transverse movement (all θ values are close to 0 or 180°). All of them give a transverse movement that is many times smaller than that at D2 pore. This indicates that D1 pore remains shut during the functional process.

3.4 Experimentally Observed Conformation Changes Validate the Predicted Functional Motions

In their work, Banerjee et al.[2] determined the atomic resolution structures of p97 at three different conformation states. They are p97 bound with ADP at both D1 and D2 sites (5FTL, conformation I), with ADP at D1 sites and ATPγS at D2 sites (5FTM, conformation II), and with ATPγS at both D1 and D2 sites (5FTN, conformation III). All three structures are axially symmetric. Experimentally observed rotations[30,40] of p97 also indicate that the motions are symmetric.

These observed conformational changes provide a validation of the functional modes predicted from conformation I (5FTL) in the last section. To this end, we listed the top 10 modes that give the largest overlap with the conformational displacement from conformation I (5FTL) to II (5FTM) or III (5TFN). The results are listed in Tables IV and V.

There are several remarkable results. First, the mode that gives the significantly larger movement at pore residues 551–552, mode 13, is found to have the largest overlap with conformational

change from 5FTL to 5FTM. This means the motion described in mode 13 is mostly along the conformational transitions of p97 and is thus indeed a functional motion. Many of the other modes that show significant D2 pore movements also are found to give large overlaps.

Second, for D1 pore, the mode that gives the largest movement at pore residue H317, mode 4, is found to have the largest overlap with the conformational change from I (5FTL) to III (5FTN). The conformational change between I and III mainly represents the swing motion of the N domain, going from a co-planar configuration with D1 domain to an "Up configuration." A close look of mode 4 shows that it mostly represents such a motion of the N domain (see movie file of mode 4 at Supplemental Information). However, mode 4 was selected in the previous section due to its largest movement at D1 pore residue His 317. Taken together, the strong correlation between the motion of HIS 317 and the N domain indicts the important role of HIS 317 in regulating the swing motion of the N domain.

Lastly, it is worth noting that the modes that have largest overlaps are all symmetric modes. While this is not totally surprising since the conformational changes are symmetric, the results show the importance of symmetric modes in the function of this protein. Symmetric modes account for only about a small percentage of the total number of the modes. The realization that functional modes are probably symmetric has helped greatly reduce the number of modes to be considered and analyzed. It is perceivable that similar thinking could be extended to some of the other symmetric systems.

In the next section, we will take a close look at mode 13, the mode that not only gives the largest movement at D2 pore residues (551–552) but also the largest overlap with the conformational change between conformations I (5FTL) and II (5FTM). Similarly, we will take a close look at mode 10 that gives the largest movement at D1 pore residue HIS 317 and has the largest overlap with the conformational change between conformations I (5FTL) and III (5FTN).

3.5 The Venous Valve Like Mechanism at D2 Pore

The functions of p97 are quite well understood. For example, it is known that it performs unfolding activities on substrates it binds and helps extract them from ERAD[31,32,39]. The pore residues have

been long recognized to have a critical functional role. However, the detailed mechanism of how p97 fulfills its tasks is less clear. By selecting the modes that give largest movement at D2 pore-1 loop (residues W551 and F552), we have identified a mode that also has largest overlap with observed conformational change. Now the advantage of using normal modes is that they reveal also the motion of the rest of the structures and potentially the functional mechanism of the whole system.

Figure 5 shows the conformations of p97 as it moves along mode 13: (A) at conformation I (5FTL), (B) where the pore is being closed up, and (C) where the pore residues move down to further open the pore. The conformation shown in (B) resembles conformation II (pdbid: 5FTM) determined in cryo-EM[2]. A movie that shows the motion of mode 13 is given in SI. Mode 13 as portrayed in the movie and Figure 5 reveals a plausible functional mechanism of p97. It describes a pulling/pumping motion of D2 as it moves downward (away from D1). While D2 domains move downward, D1 domains move upward, creating a larger volume in the chamber, like a "breathing-in" motion. As shown earlier, the volume of the chamber increases by as much as 50% when the structure goes from conformation II (5FTM, similar to Figure 5(B)) to conformation I (5FTL, Figure 5(A)). This movement also creates a larger gap at the interface between D1 and D2 domains, which we will examine later.

Figure 6 further illustrates the working mechanism of the D2 pore. The figure shows the motion patterns of pore residues (D2 pore-2 loop). Only two protomers (out of the six) are shown for clarity. The figure illustrates that as the pore residues move downwards, it gradually opens up the pore, presumably pulling the substrate downward with them. As it moves back and upward, the volume of the chamber is reduced and squeezed, preventing the substrate from going back with them, similar to what a venous valve does. The opening of at the interface between D1 and D2 also may shut, preventing substrate to slide back.

The concave regions (marked by black lines in the figure) around "the valves" (circled in Figure 6) may serve to grab or push the substrate out as it is being pulled out from the chamber.

One may ask, where does the directional preference come from? How is the substrate pulled out of the chamber through D2 pore instead of being pulled in? The answer is probably that the

downward motion of D2 is driven by ATP hydrolysis at D2 domain and is thus more forceful. After the chamber has been fully expanded, it will retract passively to its original configuration and bind ATPs, ready for a new round of actions. This process is similar inhalation (active) and exhalation (passive) in breathing.

3.6 D1 Pore Motions are Coupled With the Motions of N Domain

Now we examine mode 4. Mode 4 gives the largest movement for D1 pore residue His 317, which blocks the D1 pore. Mode 4 also has the largest overlap with the conformational change between conformation I (5FTL, ADP bound at both D1 and D2) and III (5FTN, ATP bound at both D1 and D2).

Figure 7 shows the motions of p97 as it moves along mode 4: (A) at the initial conformation, and (B) when the N domain is up. Most of the movements happen at the N domain. While N domain moves up, D1 moves down. The hinge of this movement is at the linker region between N and D1 domains (highlighted in yellow in Figure 7). During this movement, D2 domain moves only slightly, up and down. The D1 pore movement is almost strictly longitudinal along the pore, and there is little or no transverse movement. The D1 pore remains shut. It is reasonable to believe that during the functional process the up and down movement of the N domain is strongly coupled with the motion of D1 domain, but not with D2 domain. This process is probably powered by ATP hydrolysis at D1 domains, since D2 domains display little motion. Since the role of N domains is to recognize, interact, and bind with substrate proteins, it is perceivable that though D1 pore remains shut, the up and down motion of the N domain may serve to bring substrate to the interface between D1 and D2 domains, which has gaps that may allow substrates to enter into the chamber. This process, as well as the ATP hydrolysis at D1 domains, may pause after a substrate has been brought into the chamber and before it is extracted from the D2 pore. If that is the case, the D1 domain may remain at a temporarily inactive, ADP-bound state, while at D2 domain, the ATP hydrolysis is repeatedly fired to gradually pull the substrate out through the D2 pore. This is consistent with the observation that that D2 is the active ATPase domain[14] and that the D1 domain remains catalytically inactive[38].

3.7 The Role of His 317

Mutation studies[14] found that HIS 317 was important to the proper function of p97. Mutating HIS 317 to Alanine was found to impair substrate degradation[14]. It was suggested that HIS 317 serves as an "interaction nexus" for the six protomers[14]. We agree with this and propose that the role of HIS 317 is to maintain the rigidity at and near the D1 pore. The tight connection at HIS 317 ensures a near-perfect longitudinal motion of D1 pore along the pore axis and a strong coupling between the motions of D1 domain and N domain. The vertical motion of D1 pulls the N domain up! The motion of the N domain is strongly coupled with that of the D1 domain. This remarkable insight as revealed by normal modes may be more difficult to obtain by other means. This shows again the value of normal mode analysis, which is superior to most other methods in capturing important global, collective motion patterns.

A possible study we can do here is to study if H317A mutant loses the cooperativity, and if the mode that gives a strong correlation between D1 and N domains disappear after the mutation. We did this mutation and found this is indeed the case. The "swing-up" motion of N domain is no longer coupled with the longitudinal motions of the D1 pore. This may explain the loss of cooperativity (going from positive cooperativity to negative cooperativity) among the six protomers after the H317A mutation[14].

The rigid D1 pore held by HIS 317 prevents radial motions (i.e., motions that stretch open the pore). It ensures the force caused by the ATP binding and hydrolysis to be along the pore axis (longitudinal) or rotational. The longitudinal motion of the D1 pore along the pore axis pulls the N domain up.

3.8 The Hidden Entry: How Dynamics May Create Entry Ways at D1/D2 Interface

As seen in the previous section, mode 13 aligns most closely with the direction of the conformational change from conformation I (5FTL) to II (5FTM). The advantage of normal modes over static conformations is that they reveal in details how a conformational change takes place. As

intrinsic motions of a system, they are often linked to the mechanism.

In addition to revealing the working mechanism of D2 pore, this functional mode (mode 13) reveals also a way in which the substrate may enter the protein chamber. As D2 moves downward and D1 upward, it creates a larger opening between D1 and D2 interface. A channel mapping using CAVER[9] shows the clearance increases from 1.72 to 1.93 after p97 goes from conformation I to conformation III. It is possible the actual motion along mode 13 may have a larger amplitude (see section on Twisting Motions) and a larger gap may be created. It is also possible that the local structure may rearrange and a larger hole may be opened during substrate binding and that the substrate may enter into the chamber through this opening. Lastly, the twisting motions of D2 ring relative to D1 ring as addressed in the following section also may help create a larger gap.

The lining residues of the channel identified above are given in Table VI. These residues are good candidates for future mutation studies. If a bulky residue(s) is introduced that may block this entry way, will it impair the degradation of p97?

3.9 The Twisting Rotation of D2 ring relative to D1/N domains

Another important functional motion of p97 is the twisting motion of D2 relative to D1/N that was observed experimentally[2,18,30,40]. To identify such a twisting motion in normal modes, we turn to the symmetric rotational modes.

Among the modes that give the largest movement at D2 pore, another outstanding mode is mode 7. From Table II it is seen that this mode motion is mostly transverse and rotational since ϕ is close to -80°. Furthermore, since the directions of the rotations for D1 and D2 domains are opposite to each other (ϕ is 72° at D1 and -80° at D2, see Table II), it means this mode (i.e., mode 7) may represent a twisting motion between domains D1 and D2. Figure 8 and the movie file of mode 7 in SI show that indeed this is the case. Twisting motions of about 22–23 degrees have been experimentally observed in functional process of p97 using AFM[30] and cryo-EM[40]. The two most recently published structures of p97 using crystallography[18] and atomic-resolution cryo-EM[2] also confirm the existence of conformations where there is a twisting between D1 and D2, but the extent of rotation is smaller, about 14 degrees. Notice that a larger degree of movement is observed

dynamically than in static structures, suggesting that proteins can have a larger degree of motions than what is seen in the few conformations captured in crystallography or cryo-EM. Lastly, it is worth pointing out that next to mode 13, mode 7 has the largest overlap with the conformational change from conformation I to II (see Table IV).

It is foreseeable that both the pulling/pumping motion described in mode 13 and the twisting motion described by mode 7 are essential to the function of p97. Indeed, work by Wang[36] predicted that the mechanical force by ATP binding and hydrolysis should have both a parallel (along the axis, for pulling) and perpendicular component. Moreover, Wang[36] predicted the mechanical force caused by ATP binding and hydrolysis in p97 should be more along the axis and to a less extent, perpendicular to the axis (twisting). Since these two modes have different frequencies, it is likely that twisting and pulling actions are carried out in an alternating fashion, instead of a a combined spiral translocation that will be more suitable for processing single-strand or double strand DNA[36].

It was shown by Wang[36] that the mechanical force generated by ATP hydrolysis is strictly longitudinal along the pore axis for HslU[37], another protein in the AAA+ family. This aligns well with the known threading process of HslU that is straightly up and down along the pore[37]. While for p97, Wang[36] predicted that the mechanical force by ATP hydrolysis has both a longitudinal and a transverse components. In other words, twisting motion seems to be important to the function of p97. This indirectly suggests that substrates may enter into the p97 chamber in a different way from that of HslU[37], possibly through the D1/D2 interface, even though both HslU and p97 are symmetric hexamers. The twisting motion may not only help loosen up the substrate for translocation but also increase the gap at the interface between D1 and D2 domains. Again we suggest that mutagenesis studies should be performed on the residues lining the opening (see Table VI) at the D1/D2 interface.

4 Discussion

p97 is one of the molecular machines in the AAA+ family and plays an important functional role in protein degradation. Its central pore is known to be a key component in the functional process. However, the mechanism by which p97 realizes its functions remains controversial and

unclear. In this work, by applying a novel symmetry and normal mode based method and utilizing the knowledge of the importance of the central pore, we have identified key intrinsic motions of this structural complex that are closely related to its functional process. Our results thus shed new insights into the functional mechanism of this structure and provide new understandings that link molecular motions to experimental observations. Our results provide a computation-based explanation to experimental observations.

Normal modes have been widely and successfully used in interpreting conformational changes. In contrast, it is rarely used to predict conformational changes based on one single structure. To the best of our knowledge, this work may be the first case of accurately predicting functional motions based on a *single* structure using normal modes. The success comes mainly from the presumption that functional motions should give the largest movement at D1 or D2 pore residues and that functional motions are likely to be symmetric for p97. It is foreseeable that the same or similar presumption may hold true for other structure complexes and may be utilized to predict their functional motions.

Our NMA-based studies demonstrate the following:

- D2 pore is most involved in the functional process. D2 pore exhibits a venous valve like mechanism in pulling a substrate out of the chamber. The mechanism is used probably to ensure one-way movement of the substrate;

- D1 pore remains shut during the functional process. The strong interactions at and around HIS 317 residues are strong enough that it allows little radial motion at D1 pore. The motions at D1 pore are thus mostly vertical motions along the pore axis. Transversely, the motions are in a much smaller magnitude and are mostly rotational (i.e., there is none or little radial motion). This agrees with previous findings[14];

- because D1 pore remains shut and the mechanism at D2 pore allows substrate only to exit, it is likely that substrates enter the chamber through the gaps at D1/D2 interface[14]. Our results support this idea, showing that as D2 moves down and D1 moves up, it creates a bigger opening at the interface;

- the "swing-up" motion of the N domain is closely coupled with the vertical motions of the D1 pore. This insight is new and has not been observed before. Our normal modes-based study (esp. mode 7) clearly demonstrates a strong connection between the two motions;
- the twisting rotations observed in experiments[30,40] between D1 and D2 domains not only exist but also are energetically highly favorable (see section 3.9).

The Functional Cycle of p97

Taken together, we propose that the functional cycle of p97 is as follows. Initially, the system is at apo state, where the N domain lays flat and co-planar with the D1 domain. This is following by ATP binding at both D1 and D2 domains. The N domain goes from down (flat) position and up position. Note that there is probably a natural equilibrium between the two (up or down position for the N domain)[40] and ATP binding at the D1 domain probably makes the up position more favorable. N domains (there are six of them since p97 is a hexamer) identify and interact with substrates, sometimes via adaptor proteins. This is followed by ATP hydrolysis at D1 domains, which probably causes N domains to go back to the down position. This process may repeat several times before N domains successfully bring a substrate to the D1/D2 interface. From then on, D1 domains remain inactive and ADP bound until the next substrate needs to be brought in. Next, ATP hydrolysis takes place at D2 domains. D2 domains rotate relative to D1[30]. The rotation probably serves to loosen up the substrate and its contacts with the chamber and thus facilitates the subsequent pulling exerted by the downward movement of D2 pore residues. Next, D2 pore residues move downward/outward and D2 pore opens up, pulling substrate with it. After this "active breathing"-like motion, the system relaxes and resumes back to its ADP bound state (e.g., D2 rotates back relative to D1), readying itself for another round of ATP hydrolysis at the D2 domains, which may have to be repeated many times until substrate is fully pulled out of the chamber and unfolded.

Therefore, as a molecular machine, p97 performs its unfolding activity by repeatedly carry out two major mechanistic actions powered by ATP hydrolysis: *pulling* and *twisting*. The net effect is that the substrate gets twisted and pulled gradually. Interestingly, the same strategy, i.e., pulling

or twisting, is what we often use in separating one object from another. The venous valve-like mechanism employed by D2 pore to ensure one-way movement of the substrate also is remarkable. It would be interesting to see if there exist other molecular systems that utilize a similar strategy.

According to our model, D1 and D2 domains function in a step-wise fashion. D1 domains are active first and move cooperatively with N domains in fetching a target substrate. After a substrate is brought in, D1 domains become inactive and D2 domains become active. This explains previous observations that D1 and D2 rings negatively cooperate with each other and hydrolysis take place in one domain at a time[6], while the ATPase activity within the D2 domains cooperative positively[14].

An open D1 pore?

In Yeung et al.'s work using cryo-EM[40], an open D1 pore conformation at the apo state was proposed. According to the authors, "the rearrangement of individual D1 protomers with respect to the crystal structures results in an open D1 pore and a raised position of the N domains. In addition, the D2 domains show various degrees of tilt. In conformation 2, the N domains are coplanar, the D1 ring is tightly packed and the D1 pore closed."[40] On the other hand, an open D1 pore was not observed in any of the other studies. Our current study using NMA also indicates it is very difficult for D1 pore to open. How to reconcile the two?

A possible explanation is that the apo conformation with an open D1 pore proposed by Yeung et al.[40] is different from all the 13 existing p97 structures (see Table I) existing in the PDB[5], all of which has ATP or ADP bound at D1 domain and a tightly shut D1 pore. It might also be possible the open D1 pore may be an artifact of cryo-EM reconstruction, the process might have been under-constrained. However, the 3-layer architecture of p97 as proposed by the same authors[40] is right and indeed has been confirmed by the recent near-atomic resolution structures[2].

Acknowledgment

Funding from National Science Foundation (CAREER award, CCF-0953517) is gratefully acknowledged.

References

1. ATILGAN, A. R., DURELL, S. R., JERNIGAN, R. L., DEMIREL, M. C., KESKIN, O., AND BAHAR, I. 2001 Anisotropy of fluctuation dynamics of proteins with an elastic network model. *Biophys. J.*, 80(1):505–515.

2. BANERJEE, S., BARTESAGHI, A., MERK, A., RAO, P., BULFER, S. L., YAN, Y., GREEN, N., MROCZKOWSKI, B., NEITZ, R. J., WIPF, P., FALCONIERI, V., DESHAIES, R. J., MILNE, J. L., HURYN, D., ARKIN, M., AND SUBRAMANIAM, S. 2016. 2.3 Å resolution cryo-EM structure of human p97 and mechanism of allosteric inhibition. *Science* 351:871–875.

3. BARTHELME, D. AND SAUER, R. T. 2013. Bipartite determinants mediate an evolutionarily conserved interaction between Cdc48 and the 20S peptidase. *Proc. Natl. Acad. Sci. USA* 110:3327–3332.

4. BARTHELME, D. AND SAUER, R. T. 2015. Origin and functional evolution of the Cdc48/p97/VCP AAA+ protein unfolding and remodeling machine. *J. Mol. Biol.* .

5. BERMAN, H. M., WESTBROOK, J., FENG, Z., GILLILAND, G., BHAT, T. N., WEISSIG, H., SHINDYALOV, I. N., AND BOURNE, P. E. 2000. The protein data bank. *Nucleic Acids Res* 28:235–42.

6. BEURON, F., FLYNN, T. C., MA, J., KONDO, H., ZHANG, X., AND FREEMONT, P. S. 2003. Motions and negative cooperativity between p97 domains revealed by cryo-electron microscopy and quantised elastic deformational model. *J. Mol. Biol.* 327:619–629.

7. BROOKS, B. AND KARPLUS, M. 1983. Harmonic dynamics of proteins: normal modes and fluctuations in bovine pancreatic trypsin inhibitor. *Proc. Natl. Acad. Sci. USA* 80:6571–6575.

8. CHANG, L., CHEN, S., LIU, C., PAN, X., JIANG, J., BAI, X. C., XIE, X., WANG, H. W., AND SUI, S. F. 2012. Structural characterization of full-length NSF and 20S particles. *Nat. Struct. Mol. Biol.* 19:268–275.

9. CHOVANCOVA, E., PAVELKA, A., BENES, P., STRNAD, O., BREZOVSKY, J., KOZLIKOVA, B., GORA, A., SUSTR, V., KLVANA, M., MEDEK, P., BIEDERMANNOVA, L., SOCHOR, J., AND DAMBORSKY, J. 2012. CAVER 3.0: A tool for the analysis of transport pathways in dynamic protein structures. *PLoS Comput. Biol.* 8:e1002708.

10. CINIAWSKY, S., GRIMM, I., SAFFIAN, D., GIRZALSKY, W., ERDMANN, R., AND WENDLER, P. 2015. Molecular snapshots of the Pex1/6 AAA+ complex in action. *Nat. Commun.* 6:7331.

11. DAVIES, J. M., BRUNGER, A. T., AND WEIS, W. I. 2008. Improved structures of full-length p97, an AAA ATPase: implications for mechanisms of nucleotide-dependent conformational change. *Structure* 16:715–726.

12. DELABARRE, B. AND BRUNGER, A. T. 2003. Complete structure of p97/valosin-containing protein reveals communication between nucleotide domains. *Nat. Struct. Biol.* 10:856–863.

13. DELABARRE, B. AND BRUNGER, A. T. 2005. Nucleotide dependent motion and mechanism of action of p97/VCP. *J. Mol. Biol.* 347:437–452.

14. DELABARRE, B., CHRISTIANSON, J. C., KOPITO, R. R., AND BRUNGER, A. T. 2006. Central pore residues mediate the p97/VCP activity required for ERAD. *Mol. Cell* 22:451–462.

15. GARDNER, B. M., CHOWDHURY, S., LANDER, G. C., AND MARTIN, A. 2015. The Pex1/Pex6 complex is a heterohexameric AAA+ motor with alternating and highly coordinated subunits. *J. Mol. Biol.* 427:1375–1388.

16. GO, N., NOGUTI, T., AND NISHIKAWA, T. 1983. Dynamics of a small globular protein in terms of low-frequency vibrational modes. *Proc. Natl. Acad. Sci. USA* 80:3696–3700.

17. HANSON, P. I. AND WHITEHEART, S. W. 2005. AAA+ proteins: have engine, will work. *Nat. Rev. Mol. Cell Biol.* 6:519–529.

18. HÄNZELMANN, P. AND SCHINDELIN, H. 2016. Structural basis of ATP hydrolysis and intersubunit signaling in the AAA+ ATPase p97. *Structure* 24:127–139.

19. HUMPHREY, W., DALKE, A., AND SCHULTEN, K. 1996. VMD – Visual Molecular Dynamics. *J Molec Graphics* 14:33–38.

20. HUYTON, T., PYE, V. E., BRIGGS, L. C., FLYNN, T. C., BEURON, F., KONDO, H., MA, J., ZHANG, X., AND FREEMONT, P. S. 2003. The crystal structure of murine p97/VCP at 3.6 Å. *J. Struct. Biol.* 144:337–348.

21. ISHIKAWA, T., BEURON, F., KESSEL, M., WICKNER, S., MAURIZI, M. R., AND STEVEN, A. C. 2001. Translocation pathway of protein substrates in ClpAP protease. *Proc. Natl. Acad. Sci. USA* 98:4328–4333.

22. LEVITT, M., SANDER, C., AND STERN, P. S. 1983. The normal modes of a protein: Native bovine pancreatic trypsin inhibitor. *Int. J. Quant. Chem.* 10:181–199.

23. NA, H., JERNIGAN, R. L., AND SONG, G. 2015. Bridging between nma and elastic network models: Preserving all-atom accuracy in coarse-grained models. *PLoS Comput. Biol.* 11:e1004542.

24. NA, H. AND SONG, G. 2014a. Bridging between normal mode analysis and elastic network models. *Proteins* 82:2157–2168.

25. NA, H. AND SONG, G. 2014b. A natural unification of GNM and ANM and the role of inter-residue forces. *Phys. Biol.* 11:036002.

26. NA, H. AND SONG, G. 2015a. Conventional NMA as a better standard for evaluating elastic network models. *Proteins* 83:259–267.

27. NA, H. AND SONG, G. 2015b. The performance of fine-grained and coarse-grained elastic network models and its dependence on various factors. *Proteins* 83:1273–1283.

28. NA, H. AND SONG, G. 2016a. The effective degeneracy of protein normal modes. *Phys. Biol.* 13:036002.

29. NA, H., SONG, G., AND BEN-AVRAHAM, D. 2016b. Universality of vibrational spectra of globular proteins. *Phys. Biol.* 13:016008.

30. NOI, K., YAMAMOTO, D., NISHIKORI, S., ARITA-MORIOKA, K., KATO, T., ANDO, T., AND OGURA, T. 2013. High-speed atomic force microscopic observation of ATP-dependent rotation of the AAA+ chaperone p97. *Structure* 21:1992–2002.

31. OBERDORF, J., CARLSON, E. J., AND SKACH, W. R. 2006. Uncoupling proteasome peptidase and ATPase activities results in cytosolic release of an ER polytopic protein. *J. Cell Sci.* 119:303–313.

32. RABINOVICH, E., KEREM, A., FROHLICH, K. U., DIAMANT, N., AND BAR-NUN, S. 2002. AAA-ATPase p97/Cdc48p, a cytosolic chaperone required for endoplasmic reticulum-associated protein degradation. *Mol. Cell. Biol.* 22:626–634.

33. ROTHBALLER, A., TZVETKOV, N., AND ZWICKL, P. 2007. Mutations in p97/VCP induce unfolding activity. *FEBS Lett.* 581:1197–1201.

34. SIMONSON, T. AND PERAHIA, D. 1992. Normal modes of symmetric protein assemblies: Application to the tobacco mosaic virus protein disk *Biophys. J.* 61:410–427

35. TASUMI, M., TAKEUCHI, H., ATAKA, S., DWIVEDI, A. M., AND KRIMM, S. 1982. Normal vibrations of proteins: Glucagon. *Biopolymers* 21:711–714.

36. WANG, J. 2004. Nucleotide-dependent domain motions within rings of the RecA/AAA+ superfamily. *J. Struct. Biol.* 148:259–267.

37. WANG, J., SONG, J. J., SEONG, I. S., FRANKLIN, M. C., KAMTEKAR, S., EOM, S. H., AND CHUNG, C. H. 2001. Nucleotide-dependent conformational changes in a protease-associated atpase HsIU. *Structure* 9:1107–1116.

38. WANG, Q., SONG, C., AND LI, C. C. 2003. Hexamerization of p97-VCP is promoted by ATP binding to the D1 domain and required for ATPase and biological activities. *Biochem. Biophys. Res. Commun.* 300:253–260.

39. YE, Y., MEYER, H. H., AND RAPOPORT, T. A. 2001. The AAA ATPase Cdc48/p97 and its partners transport proteins from the ER into the cytosol. *Nature* 414:652–656.

40. YEUNG, H. O., FÖRSTER, A., BEBEACUA, C., NIWA, H., EWENS, C., MCKEOWN, C., ZHANG, X., AND FREEMONT, P. S. 2014. Inter-ring rotations of AAA ATPase p97 revealed by electron cryomicroscopy. *Open Biol.* 4:130142.

Figure Legends

Figure 1.

The structure of p97 (pdb-id: 5FTL). (A) A top-down view, with the six protomers in different colors. (B) A side view, with only two units shown for clarity. The N domain is in green, D1 in blue, and D2 in purple.

Figure 2.

A vertical cross section of the p97 chamber along the pore axis at conformations I (pdb-id: 5FTL), II (5FTM), and III (5FTN). The radii along the axis can be read or estimated from the grids.

Figure 3.

The symmetricity (see Eq. (3)) of all the normal modes of p97. (A) a histogram of symmetricity of the normal modes. (B) symmetricity vs. mode index.

Figure 4.

The direction of motion of a pore residue. θ is the angle between the direction of motion (black arrow) and the pore axis (red arrow). ϕ is the angle between the direction of motion projected in the X-Y plane and the radial direction. A longitudinal motion (small θ) moves the pore residue up and down, while a radial motion will stretch open or close up the pore and a tangential motion ($\theta \approx 90^\circ$

and $\phi \approx 90°$) rotates the domain. The whole structure is twisted when D1 and D2 domains are rotated in opposite directions.

Figure 5.

The conformational changes along mode 13. (A) The initial conformation as taken from 5FTL. (B) when D2 moves up, D2 pore closes up. The chamber volume decreases as both D1 and D2 domains compress in, as in a "breathing-out" motion. (C) In the opposite direction, D2 moves down and further opens up the D2 pore while D1 moves up, as in a "breathing-in" motion.

Figure 6.

The venous valve-like mechanism of the D2 pore, with the three figures shown in Figure 5 overlaid together. D2 pore-2 loop (circled) serves as "valves." The concave structure outside the valves may serve to grab or push the substrate out as it is being pulled out of the chamber.

Figure 7.

The characteristic motion along mode 4. (A) at initial conformation (taken from 5FTL). (B) when N domains are moving up. The linker region is highlighted in yellow.

Figure 8.

The twisting motion along mode 7 from a top-down view. (A) at the initial conformation taken from 5FTL. (B) when D2 (in purple) rotates counter-clockwise and D1/N (in blue and green) rotate clockwise. The extent of rotation of D2 relative of D1 as shown in the figure is about 7°. The magnitude of rotation is picked arbitrarily here since NMA modes do not have magnitude information.

Table I: A summary of existing structures of p97.

PDB-ID	res(Å)	method	species	nucleotide-bound state	oligomeric state	authors references
1R7R	3.6	X-ray	mouse	ADP	1 chain	Huyton et al.[20]
3CF1	4.4	X-ray	mouse	ADP/ADP.alfx	3 chains	Davies et al.[11]
3CF2	3.5	X-ray	mouse	ADP, AMP-PNP	4 chains	
3CF3	4.25	X-ray	mouse	ADP	3 chains	
5C18	3.3	X-ray	human	ATPγS	6 chains	Hanzelmann et al.[18]
5C19	4.2	X-ray	human	apo form	6 chains	
5C1A	3.8	X-ray	human	ATPγS	12 chains	
5C1B	3.08	X-ray	human	UFD1-SHP	6 chains	
5FTJ	2.3	cryo-EM	human	ADP	6 chains	Banerjee et al.[2]
5FTK	2.3	cryo-EM	human	ADP	6 chains	
5FTL	2.3	cryo-EM	human	ADP	6 chains	
5FTM	2.3	cryo-EM	human	ADP,ATPγS	6 chains	
5FTN	2.3	cryo-EM	human	ATPγS	6 chains	

Table II: The top 10 symmetric modes that give the largest movement (i.e., squared fluctuation, or SF) at D2 pore residues (W551 and F552). The SFs listed here are averaged SFs of the two pore residues. The angles θ and ϕ are illustrated in Fig. 4 and are computed using W551.

mode number	symmetry	SF@D2	SF-XY(θ)	radial (ϕ)	SF@D1	θ	ϕ
13	1.0	0.0661	0.00050 (5)	-32	0.0102	177	36
45	1.0	0.0060	0.0019 (148)	176	0.0118	177	27
29	0.995	0.0029	0.00002 (175)	-63	0.0038	3.0	-140
133	0.998	0.0025	0.00025 (163)	74	0.00036	169	149
41	1.0	0.0025	0.00248 (92)	170	0.00038	30	-162
7	1.0	0.0018	0.00168 (73)	-79	0.00009	70	72
63	0.993	0.0017	0.00076 (142)	-96	0.00010	88	104
71	1.0	0.0015	0.00123 (69)	112	0.00172	167	-118
247	0.986	0.0013	0.00045 (151)	-151	0.00026	40	-95
21	0.901	0.0012	0.00054 (141)	60	0.0286	3	-39

Table III: The top 10 symmetric modes that give the largest movement at D1 pore residue H317. The angles θ and ϕ are computed using H317. SF stands for squared fluctuation as in Table II.

mode number	symmetry	SF@D1	SF-XY(θ)	radial (ϕ)	SF@D2	θ	ϕ
4	1.0	0.0526	0.00005 (2)	-83	0.00099	64	139
21	0.901	0.0286	0.00007 (2)	-39	0.00121	141	60
32	1.0	0.0194	0.00006 (3)	-18	0.00089	26	174
45	0.999	0.0118	0.00003 (177)	27	0.00601	148	176
13	1.0	0.0102	0.00002 (177)	36	0.0661	5	-32
349	0.999	0.0044	0.00003 (5)	62	0.00004	30	106
29	0.995	0.0038	0.00001 (3)	-140	0.00295	175	-63
86	1.0	0.0030	0.00005 (7)	-27	0.00027	128	52
103	1.0	0.0029	0.00006 (172)	42	0.00011	64	19
71	1.0	0.0017	0.00009 (167)	-118	0.00147	69	112

Table IV: The top 10 modes that give the largest overlap with the conformational displacement from conformation I (5FTL) to conformation II (5FTM). The modes in bold have been identified earlier as functionally important (see Table II) since they give the largest movements at D2 pore residues.

mode #	freq. [cm^{-1}]	overlap	symmetricity
13	4.73	0.610	0.999
7	3.66	0.366	1.0
21	5.53	0.323	0.901
41	7.98	0.204	1.0
85	14.3	0.158	1.0
45	8.96	0.139	0.999
29	6.37	0.113	0.995
147	19.7	0.108	0.882
176	22.3	0.103	0.994
63	11.5	0.098	0.993

Table V: The top 10 modes that give the largest overlap with the conformational displacement from conformation I (5FTL) to conformation III (5FTN). The modes in bold (italic) have been identified earlier as functionally important since they give the largest movement at D1 (D2) pore residues (see Tables II and III).

mode #	freq. [cm^{-1}]	overlap	symmetricity
4	2.896	0.630	1.000
29	6.371	0.238	0.995
7	3.657	0.175	1.000
41	7.979	0.174	1.000
64	11.97	0.154	1.000
63	11.59	0.114	0.993
179	22.42	0.108	0.985
45	8.961	0.092	0.999
48	10.01	0.086	0.977
635	46.66	0.084	0.995

Table VI: The residues that line the potential channel at the D1/D2 interface. The residues common to all three conformations are in bold.

pdbid	residues
5FTL	211, **212**, 215, 245, **246**, **368**, **370**, **469**, 538, **565**, 569, 570
5FTM	**212**, **246**, 349, **368**, **370**, 371, 466, 467, **469**, **565**
5FTN	211, **212**, **246**, 348, 350, **368**, **370**, 371, 466, 467, **469**, 538, 561, **565**, 569

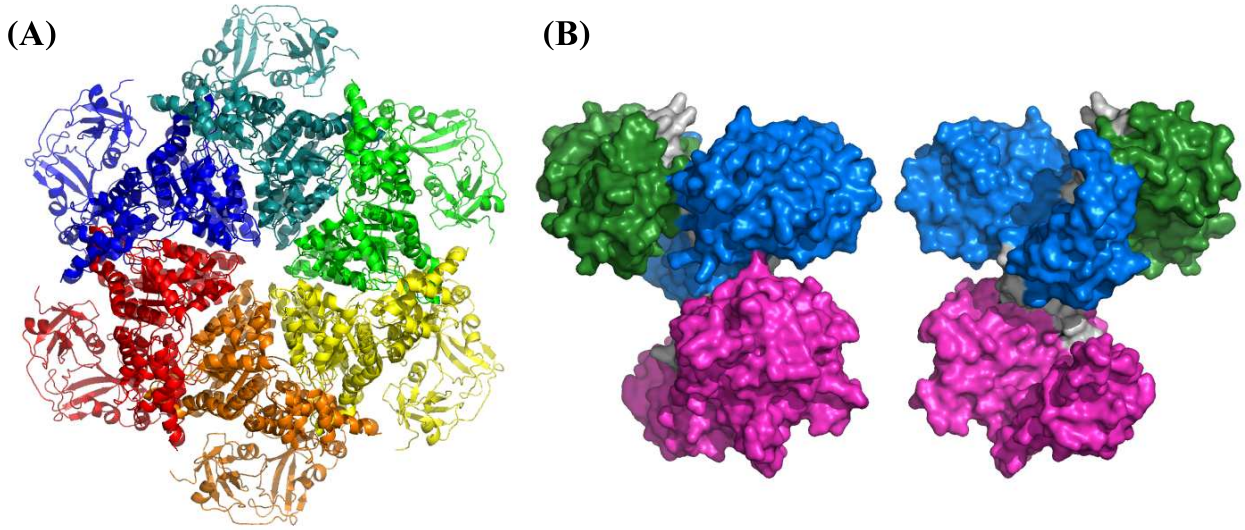

Figure 1:

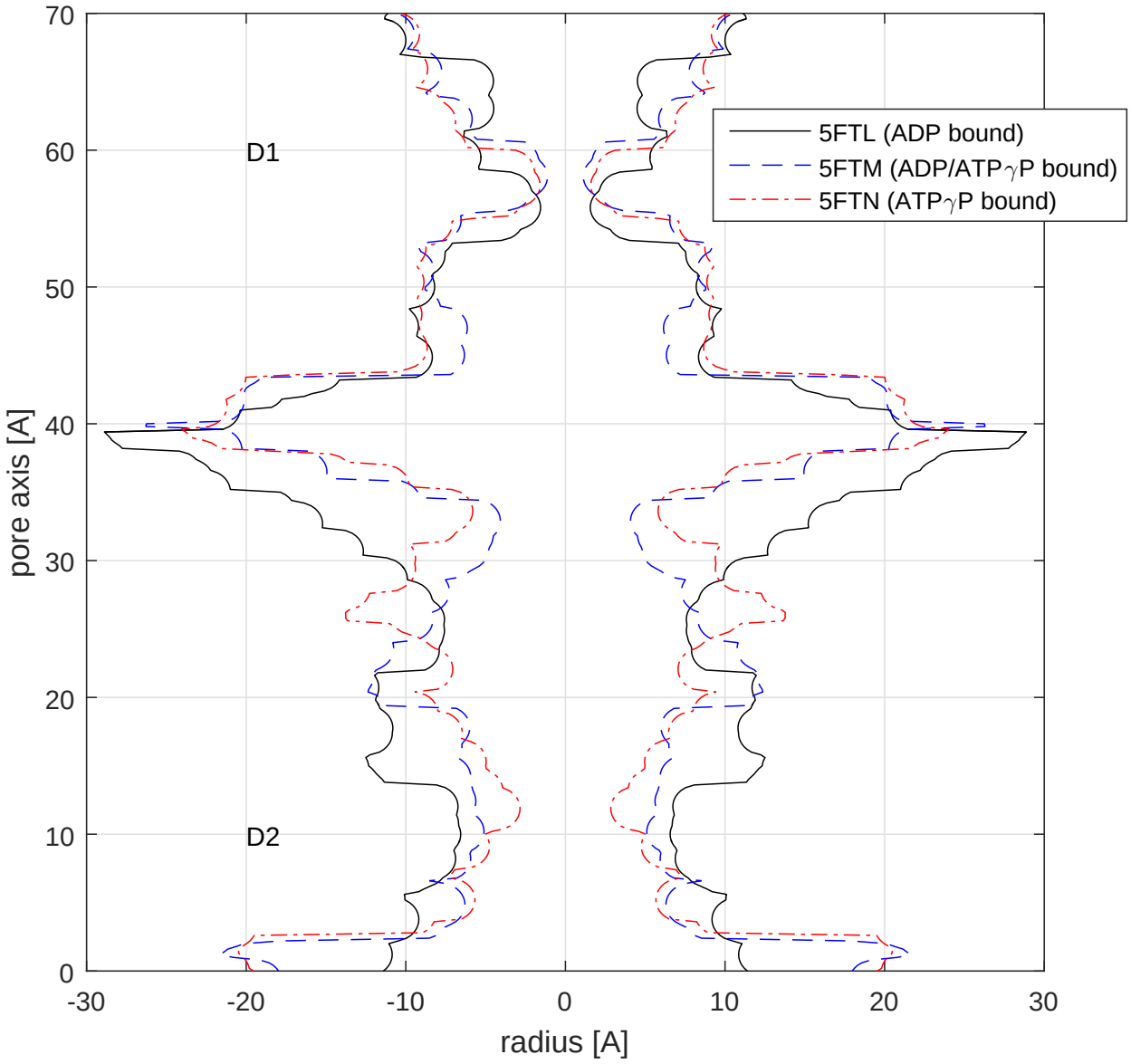
70
60
50
40
30
20
10
0
-30
-20
-10
0
10
20
30
pore axis [A]
radius [A]
D1
D2
5FTL (ADP bound)
5FTM (ADP/ATPγP bound)
5FTN (ATPγP bound)

Figure 2:

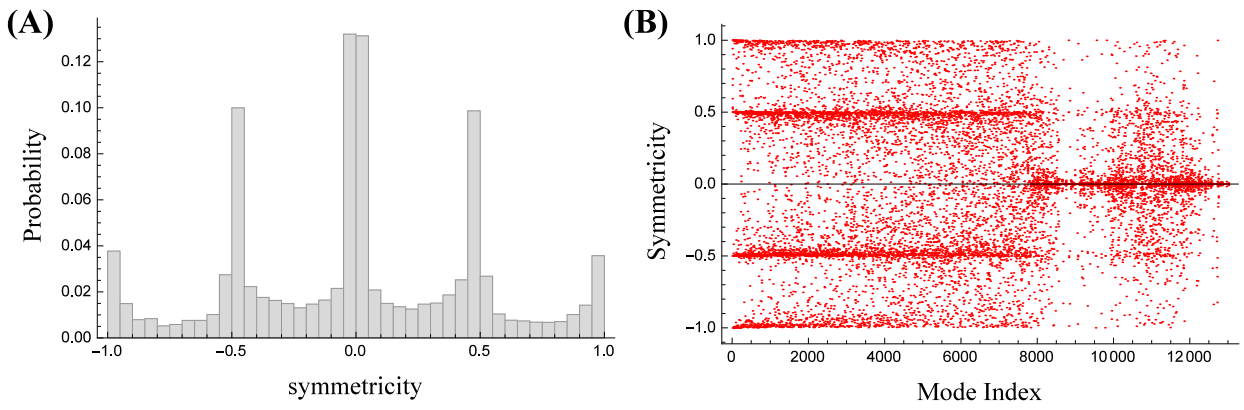
(A)
Probability
0.12
0.10
0.08
0.06
0.04
0.02
0.00
−1.0
−0.5
0.0
0.5
1.0
symmetricity
(B)
Symmetricity
1.0
0.5
0.0
−0.5
−1.0
0
2000
4000
6000
8000
10000
12000
Mode Index

Figure 3:

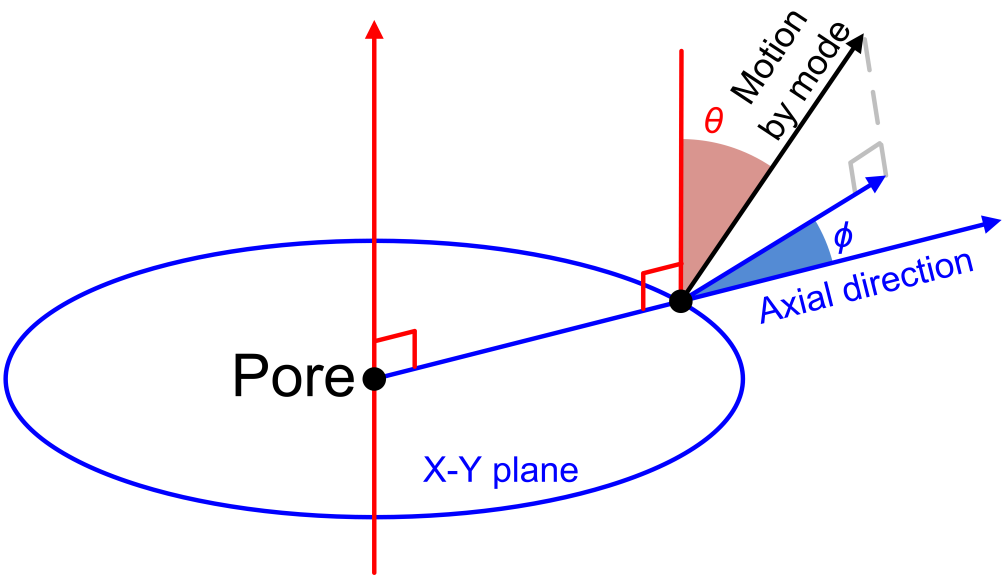

Figure 4:

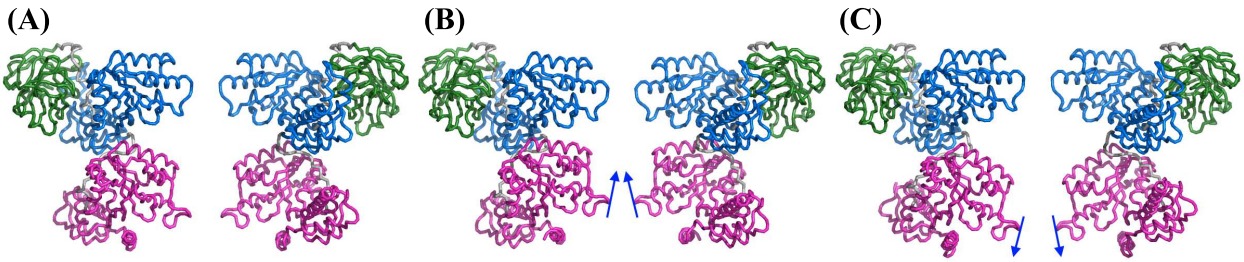

Figure 5:

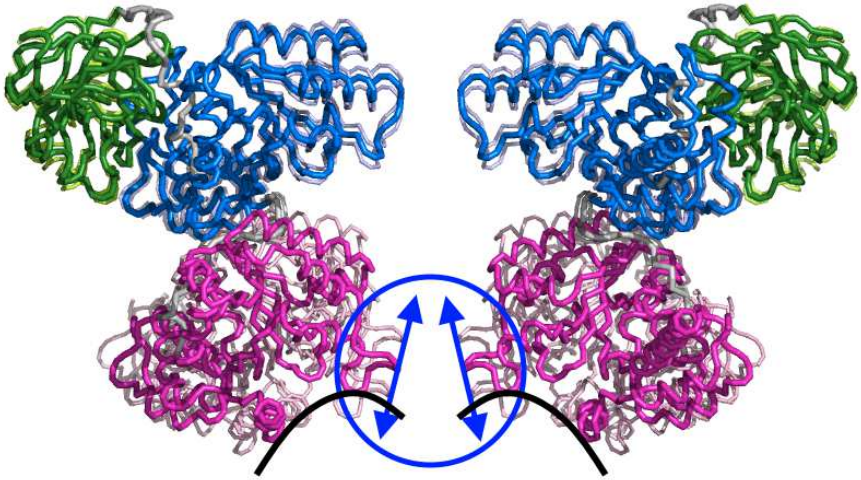

Figure 6:

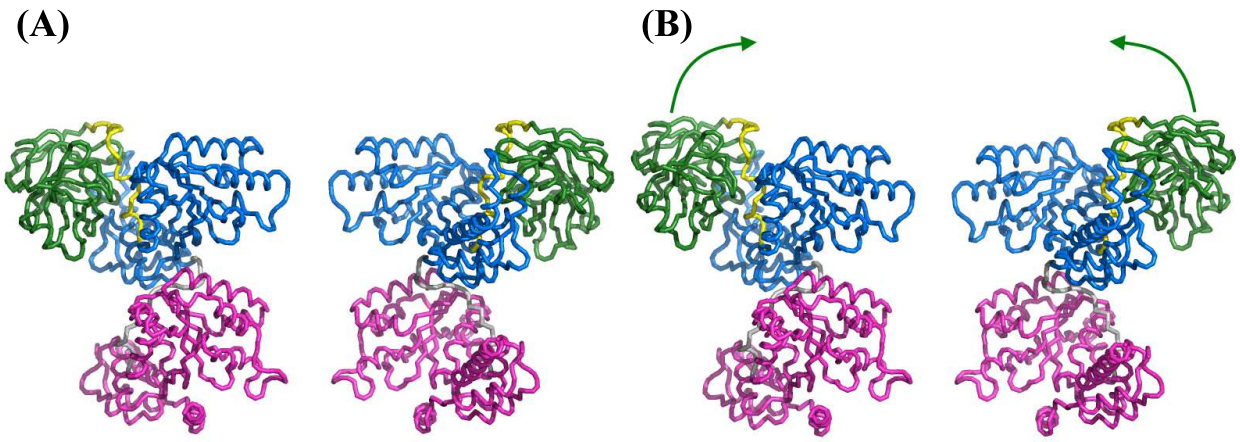

Figure 7:

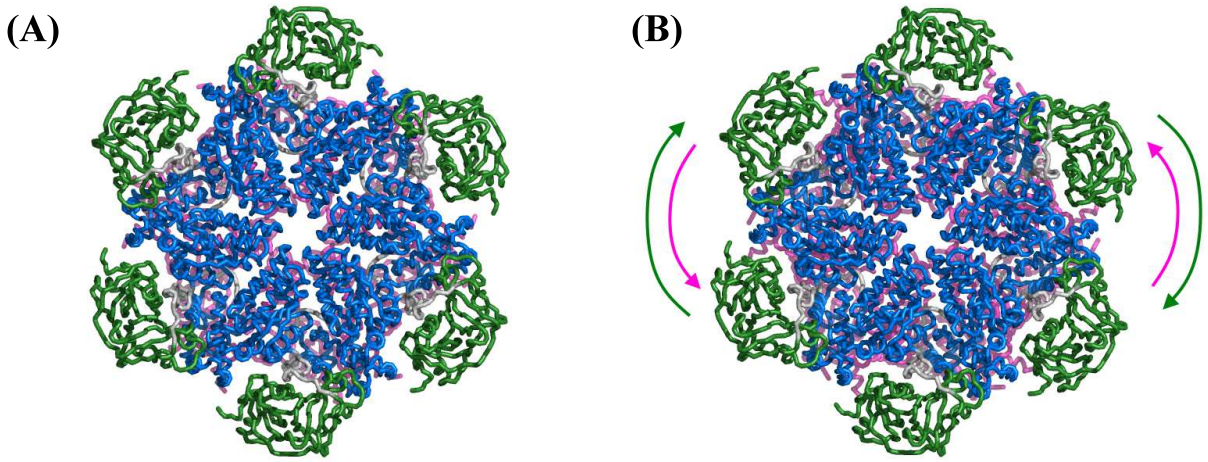

Figure 8: